Influence of atomic tip structure on the intensity of inelastic tunneling spectroscopy data analyzed by combined scanning tunneling spectroscopy, force microscopy, and density functional theory

Norio Okabayashi,[1,2,*] Alexander Gustafsson,[3] Angelo Peronio,[1] Magnus Paulsson,[3] Toyoko Arai,[2] and Franz J. Giessibl[1]

[1]*Institute of Experimental and Applied Physics, University of Regensburg, D-93053 Regensburg, Germany*
[2]*Graduate School of Natural Science and Technology, Kanazawa University, 920-1192 Ishikawa, Japan*
[3]*Department of Physics and Electrical Engineering, Linnaeus University, 391 82 Kalmar, Sweden*

Achieving a high intensity in inelastic scanning tunneling spectroscopy (IETS) is important for precise measurements. The intensity of the IETS signal can vary by up to a factor of 3 for various tips without an apparent reason accessible by scanning tunneling microscopy (STM) alone. Here, we show that combining STM and IETS with atomic force microscopy enables carbon monoxide front-atom identification, revealing that high IETS intensities for CO/Cu(111) are obtained for single-atom tips, while the intensity drops sharply for multiatom tips. Adsorption of the CO molecule on a Cu adatom [CO/Cu/Cu(111)] such that the molecule is elevated over the substrate strongly diminishes the tip dependence of IETS intensity, showing that an elevated position channels most of the tunneling current through the CO molecule even for multiatom tips, while a large fraction of the tunneling current bypasses the CO molecule in the case of CO/Cu(111).

Inelastic electron tunneling spectroscopy (IETS) with scanning tunneling microscopy (STM) is an effective method to analyze the vibrational modes of a single adsorbed molecule with subnanometer lateral resolution [1,2]. The vibrational energy of a molecule on a substrate strongly depends on the surrounding environment, such as the substrate structure and composition [3]. By studying these subtle changes of the vibrational energy using STM-IETS with a molecular-functionalized tip, it has been demonstrated that STM-IETS can provide information on the inner structure of a molecule [4,5] similarly to atomic force microscopy (AFM) [6]. These advantages of STM-IETS have accelerated research in related fields [7–16]. Owing to recent progress in the theoretical description of IETS [17–22], the qualitative understanding has been improved considerably: the symmetry of the wave functions of a tip and a molecule on a substrate and a vibrational mode of the molecule are predicted to influence the efficiency of the inelastic process (γ_{inel}) for the tunneling current involving the molecule. In order to discuss γ_{inel} on the basis of the intensity of IETS, we have to consider that IETS intensity is described by the multiplication of two factors: (1) the ratio of the tunneling current passing through a molecule to the total tunneling current ($I_{\mathrm{molecule}}/I_{\mathrm{total}}$) and (2) the efficiency of the inelastic process (γ_{inel}). These factors should in principle be affected by the geometrical structure of the substrate and of the tip.

The geometrical structure of a metal tip apex can be determined by using carbon monoxide (CO) front-atom identification (COFI) provided by AFM [23,24], where the tip apex of a force sensor is probed by a CO molecule that stands upright on a metal surface [inset of Fig. 1(e)]. The metallic tip apex atom has a dipole moment induced by the Smoluchowski effect [25], whose direction is the same as that of the CO molecule adsorbed on the surface [26]. Thus in the distance regime where the electrostatic interaction between the tip and the molecule dominates, the force between them is attractive.

When the tip is scanned over the CO molecule, this attractive force appears as a dip (smaller value) in the frequency-shift image for each atom at its apex, i.e., the number of the attractive force minima provides the number of atoms composing the tip apex [27].

In this paper, we have investigated the tip-structure-dependent IETS for individual CO molecules on a Cu surface by combining STM and AFM. We have found that a tip with a single atom on its apex (single-atom tip) gives a stronger IET signal compared with a blunt tip consisting of four atoms on the apex (four-atom tip) for a CO molecule on a Cu(111) surface. However, the intensities of the two tips become comparable when a Cu adatom is inserted between the CO molecule and the Cu(111) substrate. From these findings, we will discuss the inelastic efficiency (γ_{inel}) as dependent on the geometry of the opposite electrode, and demonstrate the validity of modern IETS theory.

The experiments were carried out in an ultrahigh-vacuum low-temperature (LT) (4.4 K) combined STM and AFM (LT-STM/AFM, Omicron Nanotechnology, Taunusstein, Germany). A Cu(111) surface was cleaned by repeated sputtering and annealing before CO molecules were adsorbed on it. The force acting between a CO molecule and the apex of the metallic tip was measured by a qPlus sensor [28]. The sensor, whose stiffness is $k = 1800 \, \mathrm{N/m}$, oscillates at $f_0 = 47375 \, \mathrm{Hz}$ with a constant amplitude of 20 pm during all STM/AFM measurements. When an average force gradient $\langle k_{\mathrm{ts}} \rangle$ acts between the tip and the CO molecule, the sensor frequency is shifted by $\Delta f = f_0 \langle k_{\mathrm{ts}} \rangle / 2k$ [29]. The current $\langle I_{\mathrm{t}} \rangle$ is averaged for many cycles of the sensor oscillation, since the bandwidth of the current amplifier is small compared to f_0. In order to measure the conductance (dI/dV) and IET signal (d^2I/dV^2), a modulation voltage (2338.7 Hz, $1 \, \mathrm{mV_{rms}}$) is added to the sample bias and the first and second harmonics in the current are detected by a lock-in amplifier (HF2LI, Zurich Instruments, Zürich, Switzerland). Throughout the whole paper, the IET signal is normalized by the differential conductance, i.e., $\mathrm{IETS} = (d^2I/dV^2)/(dI/dV)$ [10,14,18,20]. The tip is formed from an etched tungsten wire, cleaned by field evaporation and

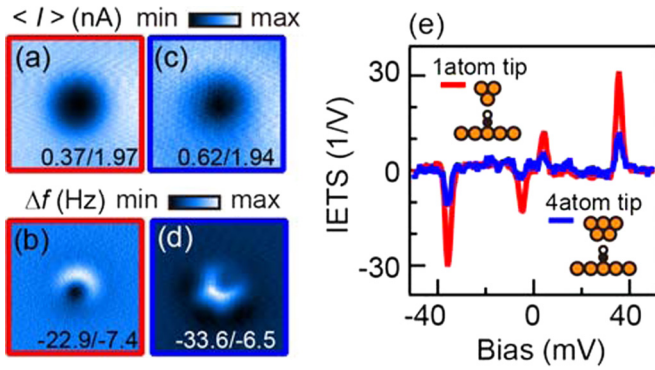*okabayashi@staff.kanazawa-u.ac.jp

FIG. 1. Constant-height current (a) [(c)] and frequency shift (b) [(d)] images (1.5×1.5 nm^2) for a CO molecule adsorbed on Cu(111) obtained with a single-atom tip (four-atom tip). The tip height is set on the Cu(111) substrate at a sample bias $V_t = -1$ mV and an average current $\langle I_t \rangle = 1.5$ nA. (e) Normalized IETS for a CO molecule at a set point of $V_t = -50$ mV and $\langle I_t \rangle = 5$ nA, where the intensity of the IETS on the Cu(111) surface is subtracted.

repeatedly poked into the Cu substrate to prepare various tip apexes [23,24,30]. The repeated poking processes probably cover the tip apex with Cu atoms. The poking processes also scatter Cu adatoms on the Cu(111) surface which are employed as another target by adsorbing a CO molecule and as an opposite electrode for the CO-functionalized tip [31].

Calculations of the IETS are performed with the density functional theory program SIESTA [32]. From the relaxed geometries obtained by SIESTA, elastic transport properties are calculated by attaching electrodes and using TRANSIESTA [33]. Vibrational frequencies and IETS are obtained from the TRANSIESTA calculations using the postprocessing package INELASTICA [34]. The SIESTA (TRANSIESTA) calculations utilize a supercell consisting of a 7- (17-) layer thick 4×4 Cu slab together with the CO molecule and a pyramidal tip modeled by four Cu atoms on the reverse side of the slab. The computations were performed using the following parameters: the Perdew-Burke-Ernzerhof functional, a 400 Ry real space cutoff, 4×4 k-points, and a double zeta, polarization (DZP) [single zeta, polarization (SZP)] basis set for CO (Cu). The IETS calculations are then performed at the Γ point.

Figure 1(a) [1(c)] shows a constant-height current image of a CO molecule on the Cu(111) surface obtained by a single-atom tip (a four-atom tip), as confirmed by the simultaneously acquired Δf image in Fig. 1(b) [1(d)]. For both tips we see the dip in the current image at the position of the CO molecule [35,36], where the current on top of the CO molecule is larger for the four-atom tip than for the single-atom tip owing to the larger tip area from which electrons can tunnel. Figure 1(e) shows the IETS for CO molecules obtained with the single-atom tip [37] and the four-atom tip, where identical current set points are used for both tips. As described in Appendix A, a background IETS measured on the copper surface is subtracted from that on the CO molecule. In the case of the single-atom tip, the frustrated translational (FT; ~ 4 meV) and frustrated rotational (FR; ~ 35 meV) modes of the CO molecule [7–9] are clearly seen in its IETS. However, the IETS intensity acquired with the four-atom tip is considerably smaller than that acquired with the single-atom tip: a 65% decrease for
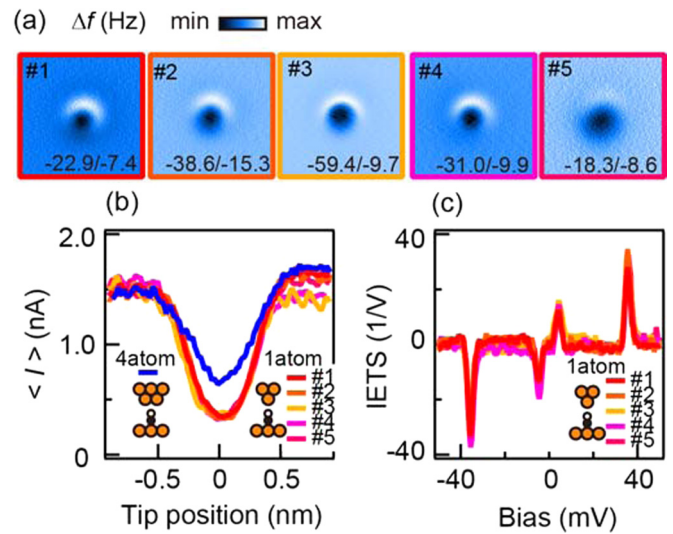

FIG. 2. (a) COFI images (1.5×1.5 nm^2) and (b) cross sections of the constant-height current images on a CO molecule with different single-atom tips (tips 1–5) at a set point of $V_t = -1$ mV and $\langle I_t \rangle = 1.5$ nA on the Cu(111) surface. As a reference, the cross section of the current image with the four-atom tip in Fig. 1(c) is added in (b). (c) IETS for CO molecules with the same tips where the set point on a CO molecule is $V_t = -50$ mV and $\langle I_t \rangle = 5$ nA.

both the FT and FR modes. A reduced IETS intensity is also observed for tips with two and three atoms on their apexes.

The strong intensity of the IETS provided by single-atom tips is confirmed by preparing different tips, which by COFI measurements [Fig. 2(a)] are single-atom tips. Cross sections of constant-height current image are shown in Fig. 2(b) [38]. Note that tip 1 is the one used in Figs. 1(a) and 1(b). In the case of tips 1 through 5, the minimum current acquired on the CO molecules is almost identical and the value is 24% of that on the Cu surface; thus these single-atom tips are judged to be sharp. The normalized IETS is also consistent for the different sharp single-atom tips (tips 1–5) [Fig. 2(c)] (Appendix A). On the other hand, the IETS intensity with a single-atom tip having secondary-atoms outside of the apex which can contribute
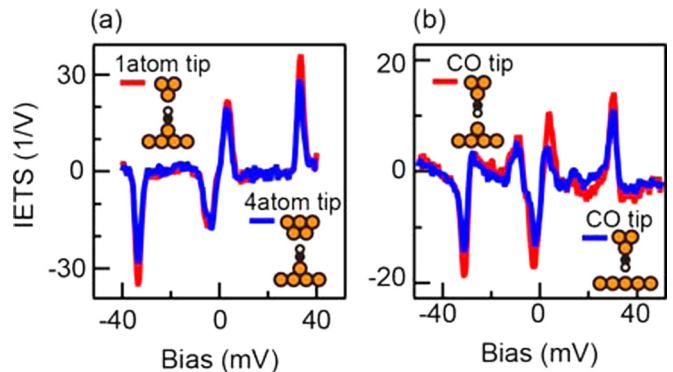

FIG. 3. (a) IETS with the single-atom tips (red) and the four-atom tip (blue) for a CO molecule on a Cu adatom. (b) IETS of a CO-functionalized tip for a Cu adatom (red) and the bare Cu(111) surface (blue). In both cases [(a) and (b)], the tip height is set at $V_t = -50$ mV and $\langle I_t \rangle = 5$ nA at the measurement position.
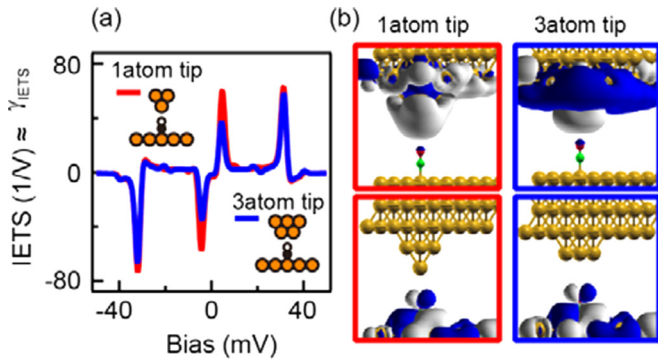
FIG. 4. (a) Calculated IETS with a single-atom tip (red) and three-atom tip (blue) for a CO molecule on Cu(111), where the tips are positioned such that the calculated elastic current is nearly identical in each case ($V_t = -50$ mV and $I_t \approx 5$ nA). Broadening by the modulation voltage (1 mV$_{rms}$) and temperature (4.4 K) is included. (b) Most important tip (upper panels) and molecular (lower panels) scattering states for the inelastic scattering by the rotational and translational modes.

to the tunneling is considerably weaker (Appendix A). This decrease originates from the increased fraction of tunneling electrons that do not interact with the CO molecule and pass directly between the tip and the substrate. The decrease in IETS intensity for the four-atom tip can be similarly rationalized as a decreased ratio of tunneling current involving the CO molecule to the total current (I_{CO}/I_{total}). To investigate how the inelastic efficiency (γ_{inel}) depends on the geometry, we now present IETS measurements for a system where the tunneling current is predominantly passing through a CO molecule.

Figure 3(a) shows IETS for a CO molecule on a Cu adatom on the Cu(111) surface (Appendix A) with the single-atom tips [37] and the four-atom tip used in Fig. 1(e), where the current set point is identical. In this case, the IETS intensity
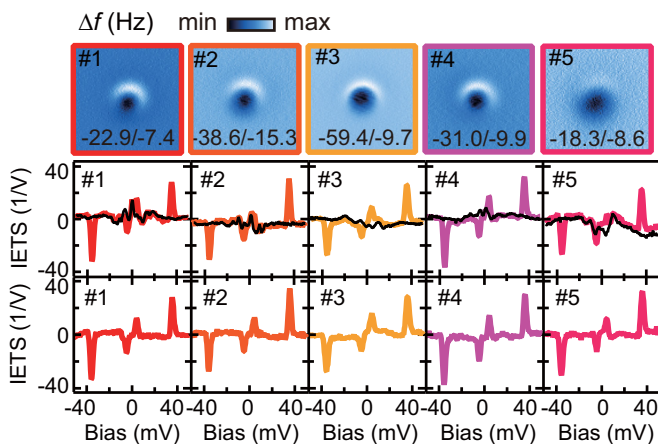

FIG. 5. Reproducibility of IETS spectra for five different tips 1–5. The data are the same shown in Fig. 2(c), but here we display the spectra individually, including the background measurements. The top row shows the constant-height frequency shift profiles (in Hz) for the five different tips. The center row displays the IETS signal in color and the background spectra in black. The bottom row displays the net IETS signal without background.

of the frustrated rotational mode with the four-atom tip is 20% smaller than in the case of the single-atom tip; however, their overall intensity is comparable. Raising the vertical position of the CO molecule by one Cu adatom strongly attenuates the direct tunneling channel between tip and substrate, causing almost all the current to pass through the CO molecule. The similarity of the intensity between the single-atom tips and the four-atom tip indicates that γ_{inel} does not depend on the tip-electrode geometry investigated here. The same conclusion can be derived from the IETS with a CO-functionalized tip over (1) a Cu adatom and (2) the bare Cu(111) surface [39]. In the two situations investigated in Fig. 3(b), tunneling electrons are emitted from or injected to the single-atom on which the CO molecule is adsorbed; thus the electron beam is focused and I_{CO}/I_{total} is expected to be large and similar. The similarity of the IETS intensity between the two cases again indicates that the structure of the opposite electrode such as the Cu adatom and Cu plane does not strongly influence the γ_{inel} for a CO molecule on the tip apex.

The role of the electrode opposite to a CO molecule in γ_{inel} has been further investigated theoretically by using the TRANSIESTA code [33]. The computations utilize a localized
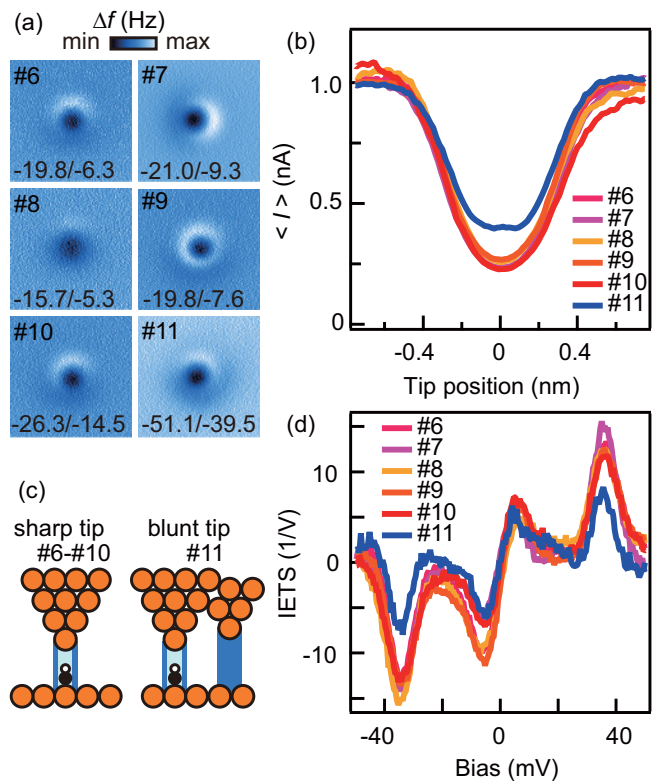

FIG. 6. (a) COFI images (1.5×1.5 nm^2) and (b) cross sections of the constant-height current images for a CO molecule with various single-atom tips (tip 6–11). The set point on the Cu(111) surface is $V_t = -1$ mV and $\langle I_t \rangle = 1.5$ nA for the COFI measurements and $V_t = -1$ mV and $\langle I_t \rangle = 1$ nA for current measurements. (c) Schematic images of the single-atom sharp and blunt tips. (d) IETS for CO molecules with the tips 6–11 where the set point on a CO molecule is $V_t = -50$ mV and $\langle I_t \rangle = 10$ nA. Note that the modulation voltage used here is 3.5 mV$_{rms}$, which is larger than the value adopted for the case of the main text (1 mV$_{rms}$).

basis set, causing the calculated tunneling current to preferentially pass through the CO molecule regardless of the opposite-electrode geometry [35], i.e., the direct tunneling between the tip and the substrate is underestimated. Thus the calculated IETS dominantly reflects the contribution of γ_{inel} rather than that of I_{CO}/I_{total}. Figure 4(a) shows the calculated IETS for a CO on a Cu (111) surface with the single- and three-atom tip. Here we can see that the intensity of IETS for the rotational mode is almost identical between two tips, which support our conclusion that the γ_{inel} does not depend on the opposite-electrode geometry.

The conclusion that γ_{inel} does not depend on the opposite-electrode geometry can be rationalized by considering the symmetry of the tip states with respect to the molecular axis [18–20]. In the case of the CO molecule, the twofold degenerate π-symmetric molecular states predominantly contribute to the inelastic tunneling process [Fig. 4(b)], because these states are more localized on the O molecule than is the σ-symmetric state [19] (Appendix B). Taking into account that the FT and FR modes have a π-symmetric character, the tip state with σ symmetry should effectively contribute to the inelastic tunneling process [Fig. 4(b)] (Appendix B). The relative contribution of the σ state to the total transmission is 50% for the three-atom tip and 57% for the single-atom tip, i.e., the contribution of the σ state drops by about 12% from a single- to a three-atom tip, resulting in an almost identical γ_{inel} in the calculation.

In contrast to the metallic tips investigated here, for the case of a CO-functionalized tip, the symmetry of the tip state is drastically changed from σ to π, which results in the inversion of the STM image contrast for a CO molecule on the Cu(111) surface from dip to bump [31,35]. This change of the tip state is predicted to decrease the efficiency of the IETS considerably for a CO molecule on a metal surface [19], in contrast to the present case.

In summary, by combining STM and AFM, we have investigated the dependence of the IETS intensity on the structure of the tip electrode for individual CO molecules for several Cu substrates. We have found that for the system where the current predominantly passes through a CO molecule that is positioned on top of a Cu adatom, the IETS intensity is almost identical regardless of the tip geometry. This result indicates that the inelastic tunneling efficiency (γ_{inel}) is independent of the geometry of the tip electrode at least for a metallic tip. This conclusion demonstrates the validity of the modern IETS theory based on density functional theory and nonequilibrium Green's functions [18–20]. While we have found that single-atom tips provide a maximal IETS intensity and great reproducibility, single-atom tips are more reactive than multiatom tips [23,24,40]. Therefore multiatom tips may still be useful in cases where a high intensity is not key but a low perturbation to the vibrating molecule by the force field of a tip is desired.
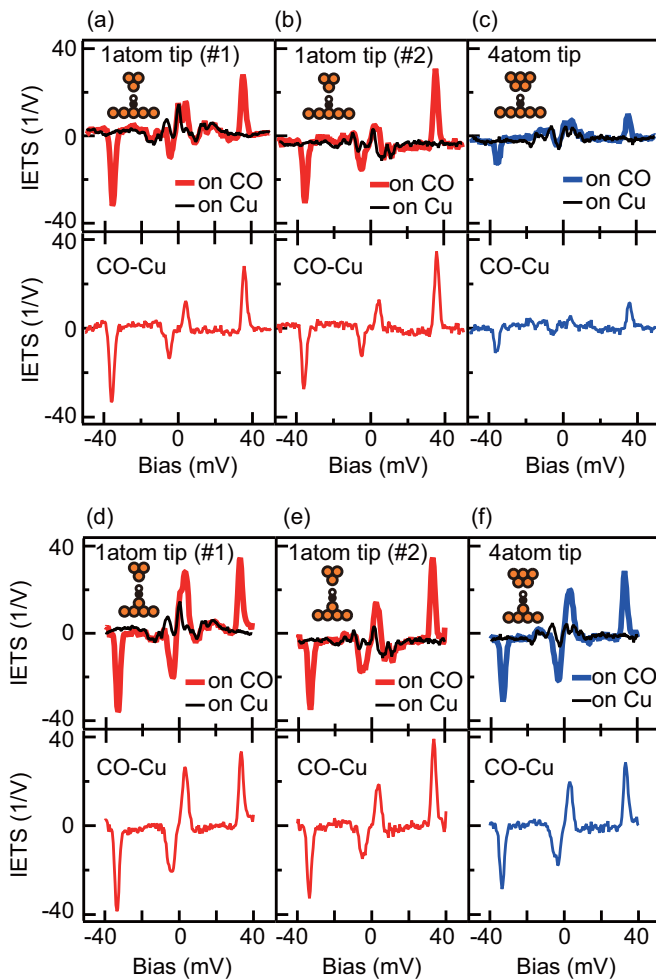
FIG. 7. Set of IET spectra on the CO molecule and the Cu(111) substrate (upper panel) and after the background subtraction (lower panel). Experimental conditions: the single-atom tip [tip 1 (2)] in (a) [(b)] for CO/Cu(111) and in (d) [(e)] for CO/Cu/Cu(111); the four-atom tip in (c) CO/Cu(111) and in (f) CO/Cu/Cu(111). For the background measurements, IET spectra on the Cu(111) surface are measured and averaged for 16 different points. A set point of $V_t = -50\,mV$ and $\langle I_t \rangle = 5\,nA$ on the CO molecule has been used for all measurements.
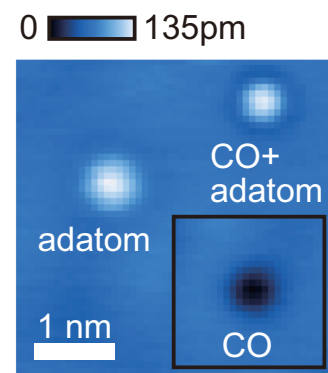

FIG. 8. Constant-current images of a Cu adatom and a CO molecule on a Cu adatom obtained with a single-atom tip ($V_t = -10\,mV$, $\langle I_t \rangle = 100\,pA$). The inset shows a CO molecule on the Cu(111) surface.
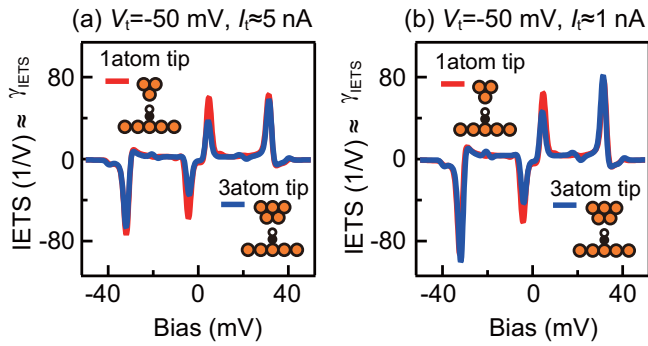
FIG. 9. Calculated IETS data compared for a single-atom tip and a three-atom tip displayed for two different set points where the transmission acquired by TRANSIESTA is almost identical between the single-atom- and three-atom tips: $V_t = -50$ mV, $I_t \approx 5$ nA and $V_t = -50$ mV, $I_t \approx 1$ nA. Note that Fig. 4(a) in the paper shows the data for the former set point.
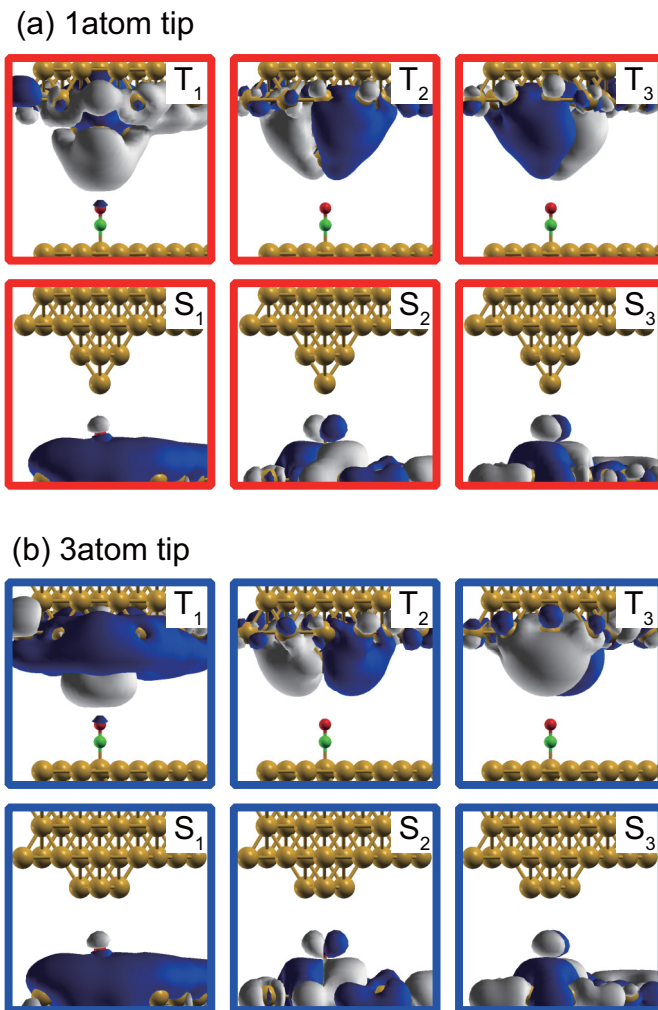
(a) 1atom tip

(b) 3atom tip

FIG. 10. Isosurface plot of the three most transmitting eigen-channels between the CO molecule on the Cu(111) surface and (a) the single-atom tip [(b) the three-atom tip] at a set point of $V_t = -50$ mV, $I_t \approx 5$ nA. The top (bottom) row of scattering states originates from the tip (substrate) side.

APPENDIX A: COMPLETE SET OF IETS WITH RELATED STM IMAGES

Figure 5 displays IETS data from five different tips. All these tips are single-atom tips, although none of them shows a COFI image that is perfectly symmetric with respect to rotations around the z axis. Instead, the COFI images show slight asymmetries that could be attributed to a slight tilt of the plane of the second atomic layer of the tip. Nevertheless, the IET spectra are essentially identical after background subtraction.

Decreased IETS intensity for the single-atom, blunt tip is shown in Fig. 6 with the data from single-atom sharp tips, where the tip apex geometry is confirmed by COFI [Fig. 6(a)] and the sharpness of the tip apex is confirmed by the constant-height current measurement [Fig. 6(b)]. When the tip is blunt, i.e., the tip constitutes a single-atom on its apex but has secondary-atoms outside of the apex [Fig. 6(c)], the IETS intensity is considerably decreased [Fig. 6(d)].

The complete set of IETS measurements for the CO molecule on a Cu adatom and a Cu substrate is shown in Fig. 7: IETS for (a) [(b)] CO/Cu(111) and (d) [(e)] CO/Cu adatom with the single-atom tip 1 (2), and for (c) CO/Cu(111)

TABLE I. Average (over two degenerate vibrations) partial contribution (%) of each scattering state (see Fig. 10) in the inelastic processes of the FT and FR modes with the elastic transmission for the single-atom and three-atom tips at a set point of $V_t = -50$ mV, $I_t \approx 5$ nA.

One-atom tip		$T_1(\sigma)$	$T_2(\pi)$	$T_3(\pi)$
	$S_1(\sigma)$	0.19	1.57	1.63
FT (%)	$S_2(\pi)$	46.65	0.01	0.10
	$S_3(\pi)$	44.64	0.01	0.07
	$S_1(\sigma)$	0.27	2.00	1.95
FR (%)	$S_2(\pi)$	48.00	0.02	0.12
	$S_3(\pi)$	46.32	0.02	0.07
Transmission $\times 10^{-4}$		9.00	3.37	3.29
Transmission (%)		57	22	21
Three-atom tip		$T_1(\sigma)$	$T_2(\pi)$	$T_3(\pi)$
	$S_1(\sigma)$	0.09	3.36	3.33
FT (%)	$S_2(\pi)$	45.17	0.16	0.08
	$S_3(\pi)$	43.78	0.08	0.15
	$S_1(\sigma)$	0.16	6.22	6.53
FR (%)	$S_2(\pi)$	37.63	0.11	0.20
	$S_3(\pi)$	35.37	0.31	0.85
Transmission $\times 10^{-4}$		8.49	4.27	4.20
Transmission (%)		50	25	25

and (f) CO/Cu adatom with the four-atom tip. The topographic image of a CO molecule on a Cu adatom is shown in Fig. 8 with the image of a CO molecule and a Cu adatom on the Cu(111) surface.

APPENDIX B: DETAILS OF THE THEORETICAL IETS

Theoretical IETS between two different set points are shown in Fig. 9, where we see that the intrinsic IETS depends weakly on the tip apex geometry. The three most transmitting eigenchannels are shown in Fig. 10 for (a) the single-atom and (b) the three-atom tip, whose contribution to the inelastic tunneling process for the FT and FR modes is summarized in Table I. We see that the contribution of the σ-symmetric state at

TABLE II. Vibrational energy (meV) of FT and FR modes at a set point of $V_t = -50$ mV, $I_t \approx 5$ nA, which are calculated by allowing the CO molecule and the one (three) Cu atoms of the one- (three-)atom tip to move (dynamical region).

	FT1	FT2	FR1	FR2
One-atom tip	4.59	4.61	31.6	31.8
Three-atom tip	4.25	4.28	31.7	31.9

the tip to the transmission is similar between the single-atom (57%) and three-atom (50%) tips, which results in similar intrinsic IETS intensity. The calculated vibrational energies are summarized in Table II.

[1] W. Ho, J. Chem. Phys. **117**, 11033 (2002).
[2] B. C. Stipe, M. A. Rezaei, and W. Ho, Science **280**, 1732 (1998).
[3] H. J. Lee and W. Ho, Phys. Rev. B **61**, R16347 (2000).
[4] C. L. Chiang, C. Xu, Z. Han, and W. Ho, Science **344**, 885 (2014).
[5] P. Hapala, R. Temirov, F. S. Tautz, and P. Jelínek, Phys. Rev. Lett. **113**, 226101 (2014).
[6] L. Gross, F. Mohn, N. Moll, P. Liljeroth, and G. Meyer, Science **325**, 1110 (2009).
[7] L. J. Lauhon and W. Ho, Phys. Rev. B **60**, R8525 (1999).
[8] A. J. Heinrich, C. P. Lutz, J. A. Gupta, and D. M. Eigler, Science **298**, 1381 (2002).
[9] L. Vitali *et al.*, Nano Lett. **10**, 657 (2010).
[10] N. Okabayashi, M. Paulsson, H. Ueba, Y. Konda, and T. Komeda, Phys. Rev. Lett. **104**, 077801 (2010).
[11] N. Okabayashi, M. Paulsson, H. Ueba, Y. Konda, and T. Komeda, Nano Lett. **10**, 2950 (2010).
[12] N. Okabayashi, M. Paulsson, and T. Komeda, Prog. Surf. Sci. **88**, 1 (2013).
[13] H. Gawronski and K. Morgenstern, Phys. Rev. B **89**, 125420 (2014).
[14] K. J. Franke, G. Schulze, and J. I. Pascual, J. Phys. Chem. Lett. **1**, 500 (2010).
[15] M. Grobis, K. H. Khoo, R. Yamachika, X. Lu, K. Nagaoka, S. G. Louie, H. Kato, and H. Shinohara, Phys. Rev. Lett. **94**, 136802 (2005).
[16] K. Motobayashi, Y. Kim, H. Ueba, and M. Kawai, Phys. Rev. Lett. **105**, 076101 (2010).
[17] N. Lorente and M. Persson, Phys. Rev. Lett. **85**, 2997 (2000).
[18] M. Paulsson, T. Frederiksen, H. Ueba, N. Lorente, and M. Brandbyge, Phys. Rev. Lett. **100**, 226604 (2008).
[19] A. Garcia-Lekue, D. Sanchez-Portal, A. Arnau, and T. Frederiksen, Phys. Rev. B **83**, 155417 (2011).
[20] E. T. R. Rossen, C. F. J. Flipse, and J. I. Cerda, Phys. Rev. B **87**, 235412 (2013).

[21] G. Teobaldi, M. Penalba, A. Arnau, N. Lorente, and W. A. Hofer, Phys. Rev. B **76**, 235407 (2007).
[22] A. Troisi and M. A. Ratner, Phys. Rev. B **72**, 033408 (2005).
[23] J. Welker and F. J. Giessibl, Science **336**, 444 (2012).
[24] T. Hofmann, F. Pielmeier, and F. J. Giessibl, Phys. Rev. Lett. **112**, 066101 (2014).
[25] R. Smoluchowski, Phys. Rev. **60**, 661 (1941).
[26] M. Schneiderbauer, M. Emmrich, A. J. Weymouth, and F. J. Giessibl, Phys. Rev. Lett. **112**, 166102 (2014).
[27] M. Emmrich *et al.*, Science **348**, 308 (2015).
[28] F. J. Giessibl, Appl. Phys. Lett. **76**, 1470 (2000).
[29] F. J. Giessibl, Phys. Rev. B **56**, 16010 (1997).
[30] M. Emmrich, M. Schneiderbauer, A. J. Weymouth, N. Okabayashi, and F. J. Giessibl, Phys. Rev. Lett. **114**. 146101 (2015).
[31] L. Bartels, G. Meyer, and K. H. Rieder, Appl. Phys. Lett. **71**, 213 (1997).
[32] J. M. Soler *et al.*, J. Phys.: Condens. Matter **14**, 2745 (2002).
[33] M. Brandbyge, J. L. Mozos, P. Ordejón, J. Taylor, and K. Stokbro, Phys. Rev. B **65**, 165401 (2002).
[34] T. Frederiksen, M. Paulsson, M. Brandbyge, and A. P. Jauho, Phys. Rev. B **75**, 205413 (2007).
[35] A. Gustafsson and M. Paulsson, Phys. Rev. B **93**, 115434 (2016).
[36] R. K. Tiwari, D. M. Otalvaro, C. Joachim, and M. Saeys, Surf. Sci. **603**, 3286 (2009).
[37] The data are an average of IETS obtained with the tip in Fig. 1(b) [tip 1 in Fig. 2(a)] and the tip 2 in Fig. 2(a), since these two tips are adopted for IETS measurements of CO/Cu/Cu(111) in addition to CO/Cu(111).
[38] The current on the Cu(111) surface is slightly modulated depending on the substrate position owing to the standing waves. The averaged current $\langle I_t \rangle$ in Fig. 2(b) is normalized such that the current on the leftmost position is 1.5 nA.
[39] The tip before the CO functionalization has a single atom on its apex, and is sharp in the sense of Fig. 2.
[40] T. Hofmann, F. Pielmeier, and F. J. Giessibl, Phys. Rev. Lett. **115**, 109901 (2015).